Eur Phys J C **33**, s01, s469–s471 (2004)
Digital Object Identifier (DOI) 10.1140/epjcd/s2003-03-431-7

EPJ C direct
electronic only

Predictions for top quark spin correlations at the Tevatron and the LHC at next-to-leading order in α_s

A. Brandenburg

Institut für Theoretische Physik E, RWTH Aachen, D-52056 Aachen, Germany

Received: 22 October 2003 / Accepted: 4 November 2003 /
Published Online: 7 November 2003 –

Abstract. Predictions for angular distributions of top quark decay products that are sensitive to $t\bar{t}$ spin correlations are presented at next-to-leading order in α_s for the Tevatron and the LHC.

PACS. 12.38.Bx Perturbative calculations – 13.88.+e Polarization in interactions and scattering – 14.65.Ha Top quarks

1 Introduction

One of the striking features of the top quark is that due to its extremely short lifetime it cannot form hadronic bound states. The strong interactions involved in the dynamics of top quark production and decay are thus reliably described by perturbative QCD. The Standard Model main decay mode $t \to Wb$ is parity violating. Therefore, the spin properties of top quarks are transferred to its decay products without being diluted by hadronization, and they become additional observables to study the interactions of the top quark. Spin observables are useful to provide constraints on fundamental parameters of the SM (e.g. V_{tb}), to probe possible new production mechanisms for top quarks, to search for non-standard couplings in top quark decays, and to test discrete symmetries (like CP). At hadron colliders, the top quarks are produced predominantly in pairs via pure QCD processes. Since QCD preserves parity, the top quarks and antiquarks produced in the parton processes $q\bar{q} \to t\bar{t}, gg \to t\bar{t}$ are unpolarized at leading order in α_s. At next-to-leading order (NLO), absorptive parts in the scattering amplitudes of the above parton reactions lead to a nonzero polarization of the top quarks and antiquarks perpendicular to the event plane. It is a quite small effect, of the order of a percent [1,2]. Much larger are the correlations of the spins of top quark and antiquark: In fact, provided one chooses an adequate spin basis, the correlations are of the order of 1. They can be studied by measuring double differential angular distributions of top quark decay products both at the Tevatron and at the LHC. In this talk, results for these distributions at NLO in the strong coupling α_s will be discussed.

2 Theoretical framework

We consider here the following processes:

$$h_1 h_2 \to t\bar{t} + X \to \begin{cases} \ell^+\ell'^- & + X \\ \ell^\pm j_{\bar{t}(t)} & + X \\ j_t j_{\bar{t}} & + X \end{cases}, \qquad (1)$$

where $h_{1,2} = p, \bar{p}$; $\ell = e, \mu, \tau$, and j_t ($j_{\bar{t}}$) denote jets originating from hadronic t ($\bar{t}$) decays. An observable that is intimately related to the $t\bar{t}$ spin correlations in the above reactions is the double differential angular distribution of the top decay products, e.g. for the dilepton channel:

$$\frac{1}{\sigma}\frac{d^2\sigma}{d\cos\theta_+ d\cos\theta_-} = \frac{1}{4}(1 - C\cos\theta_+\cos\theta_-). \qquad (2)$$

In (2), $\theta_\pm$ are the angles between the $\ell^\pm$ direction of flight in the $t(\bar{t})$ rest frame (defined by a rotation-free boost from the parton c.m.s.) with respect to axes $\hat{\mathbf{a}}$ ($\hat{\mathbf{b}}$) which will be specified below. For our choices of $\hat{\mathbf{a}}$, $\hat{\mathbf{b}}$, terms linear in $\cos\theta_\pm$ are absent in (2) due to parity invariance of QCD.

The calculation of the distribution (2) at NLO QCD simplifies enormously in the leading pole approximation (LPA), which amounts to expanding the full amplitudes for (1) around the complex poles of the t and $\bar{t}$ propagators. Only the leading pole terms are kept in this expansion, i.e. one neglects terms of order $\Gamma_t/m_t \approx 1\%$. Within the LPA, the radiative corrections can be classified into factorizable and non-factorizable [3] contributions. The impact of the non-factorizable contributions will be discussed elsewhere [4]. Here we consider only the factorizable corrections. For these the coefficient in the distribution (2) factorizes:

$$C = \kappa_+\kappa_- D. \qquad (3)$$

In (3), D is the $t\bar{t}$ double spin asymmetry

$$D = \frac{N(\uparrow\uparrow) + N(\downarrow\downarrow) - N(\uparrow\downarrow) - N(\downarrow\uparrow)}{N(\uparrow\uparrow) + N(\downarrow\downarrow) + N(\uparrow\downarrow) + N(\downarrow\uparrow)}, \tag{4}$$

where $N(\uparrow\uparrow)$ denotes the number of $t\bar{t}$ pairs with t ($\bar{t}$) spin parallel to the reference axis $\hat{\mathbf{a}}$ ($\hat{\mathbf{b}}$) etc. The directions $\hat{\mathbf{a}}$ and $\hat{\mathbf{b}}$ can thus be identified with the spin quantization axes for t and $\bar{t}$, and D directly reflects the strength of the correlation between the t and $\bar{t}$ spins for the chosen axes. In fact, a simple calculation shows

$$D = \mathrm{corr}(\hat{\mathbf{a}} \cdot \mathbf{S}_t, \hat{\mathbf{b}} \cdot \mathbf{S}_{\bar{t}}), \tag{5}$$

where $\mathbf{S}_{t(\bar{t})}$ denotes the spin operator of the top quark (antiquark) and $\mathrm{corr}(O_1, O_2)$ is the correlation of two observables defined in the standard way.

The prefactor $\kappa_\pm$ in (3) is the spin analysing power of the charged lepton in the decay $t(\bar{t}) \to b(\bar{b})\ell^\pm\nu(\bar{\nu})$ defined by the decay distribution

$$\frac{1}{\Gamma}\frac{d\Gamma}{d\cos\vartheta_\pm} = \frac{1 \pm \kappa_\pm \cos\vartheta_\pm}{2}, \tag{6}$$

where $\vartheta_\pm$ is the angle between the t ($\bar{t}$) spin and the $\ell^\pm$ direction of flight. It is clear that the value of $\kappa_\pm$ is crucial for the experimental determination of the $t\bar{t}$ spin correlations. From [5] we obtain

$$\kappa_+ = \kappa_- = 1 - 0.015\alpha_s, \tag{7}$$

which means that the charged lepton serves as a perfect analyser of the top quark spin. For hadronic decays $t \to bq\bar{q}'$ one has a decay distribution analogous to (6) (and a double angular distribution analogous to (2)), and the spin analysing power of jets can be defined. To order α_s [6] (and using $\alpha_s(m_t) = 0.108$),

$$\kappa_b = -0.408 \times (1 - 0.340\alpha_s) = -0.393, \tag{8}$$

$$\kappa_j = +0.510 \times (1 - 0.654\alpha_s) = +0.474, \tag{9}$$

where κ_j is the analysing power of the least energetic non-b-quark jet. Note that the loss of analysing power using hadronic final states is overcompensated by the gain in statistics and in efficiency to reconstruct the t ($\bar{t}$) rest frames.

To compute D at NLO QCD, the differential cross sections for the following parton processes are needed to order α_s^3, where the full information on the t and $\bar{t}$ spins has to be kept:

$$q\bar{q} \to t\bar{t},\ t\bar{t}g;\ gg \to t\bar{t},\ t\bar{t}g;\ q(\bar{q})g \to t\bar{t}q(\bar{q}). \tag{10}$$

Results at NLO QCD for the $\overline{\mathrm{MS}}$ subtracted parton cross sections $\hat{\sigma}$ for the above processes with $t\bar{t}$ spins summed over have been obtained in [7,8], while

$$\hat{\sigma}\hat{D} = \hat{\sigma}(\uparrow\uparrow) + \hat{\sigma}(\downarrow\downarrow) - \hat{\sigma}(\uparrow\downarrow) - \hat{\sigma}(\downarrow\uparrow) \tag{11}$$

has been computed for different spin quantization axes in [9,10]. This combination of spin-dependent parton cross sections can be written as follows

$$\hat{\sigma}\hat{D} = \frac{\alpha_s^2}{m_t^2}\left\{g^{(0)}(\eta) + 4\pi\alpha_s\mathcal{G}^{(1)}\right\}, \tag{12}$$

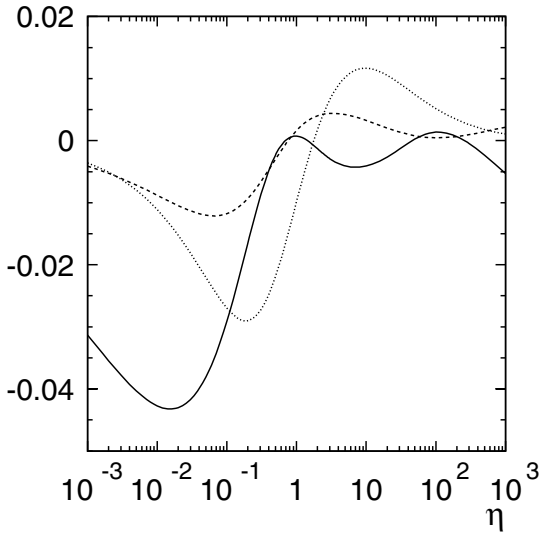

Fig. 1. Dimensionless scaling functions $g^{(0)}(\eta)$ (*full*), $g^{(1)}(\eta)$ (*dotted*), and $\tilde{g}^{(1)}(\eta)$ (*dashed*) that determine $\hat{\sigma}\hat{D}$ in the beam basis for the gg initial state

with

$$\mathcal{G}^{(1)} = g^{(1)}(\eta) + \tilde{g}^{(1)}(\eta)\ln\left(\frac{\mu^2}{m_t^2}\right), \tag{13}$$

where $\eta = \hat{s}/(4m_t^2) - 1$, and we use a common scale μ for the renormalization and factorization scale. As an example, Fig. 1 shows, for the parton process $gg \to t\bar{t}(g)$, the three functions that determine $\hat{\sigma}\hat{D}$ for the beam basis, i.e. both $\hat{\mathbf{a}}$ and $\hat{\mathbf{b}}$ are chosen to be along one of the hadron beams in the laboratory frame. Apart from the beam basis we also consider the helicity basis, where $\hat{\mathbf{a}}$ ($\hat{\mathbf{b}}$) is chosen to be the t ($\bar{t}$) direction of flight in the parton c.m.s. , and the so-called off-diagonal basis [11], which is defined by the requirement that $\hat{\sigma}(\uparrow\downarrow) = \hat{\sigma}(\downarrow\uparrow) = 0$ for the process $q\bar{q} \to t\bar{t}$ at tree level.

3 Predictions for the Tevatron and the LHC

In Table 1 we list our predictions [4,12] for the spin correlation coefficient C in the double differential distribution (2) at the Tevatron for the three different choices of spin quantization axes discussed above. We use the CTEQ6L (LO) and CTEQ6M (NLO) parton distribution functions (PDFs) [13]. Numbers are given for the dilepton, lepton+jet and all-hadronic decay mode of the $t\bar{t}$ pair, where in the latter two cases the least energetic non-b-quark jet was used as spin analyser. One sees that the spin correlations are largest in the beam and off-diagonal basis. The QCD corrections reduce the LO results for the coefficients C by about 10% to 30%.

For the LHC it turns out that the spin correlations w.r.t. the beam and off-diagonal basis are quite small due to a cancellation of contributions from the gg and $q\bar{q}$ initial states. Here, the helicity basis is a good choice, and Table 2 lists our results for the C coefficient in that case. The QCD

Table 1. Results for the spin correlation coefficient C of the distribution (2) at LO and NLO for $p\bar{p}$ collisions at $\sqrt{s} = 1.96$ TeV for different $t\bar{t}$ decay modes. The PDFs CTEQ6L (LO) and CTEQ6M (NLO) of [13] were used, and $\mu = m_t = 175$ GeV

		dilepton	lepton+jet	jet+jet
$C_{\rm hel}$	LO	−0.471	−0.240	−0.123
	NLO	−0.387	−0.185	−0.088
$C_{\rm beam}$	LO	0.928	0.474	0.242
	NLO	0.801	0.382	0.182
$C_{\rm off}$	LO	0.937	0.478	0.244
	NLO	0.808	0.385	0.183

Table 2. Results for $C_{\rm hel}$ for pp collisions at $\sqrt{s} = 14$ TeV using the same PDFs and parameters as in Table 1

		dilepton	lepton+jet	jet+jet
$C_{\rm hel}$	LO	0.319	0.163	0.083
	NLO	0.322	0.156	0.076

Table 3. Spin correlation coefficients at NLO for different PDFs for $p\bar{p}$ at $\sqrt{s} = 1.96$ TeV (upper part) and pp at $\sqrt{s} = 14$ TeV (lower part) for dilepton final states

Tevatron			
	CTEQ6M	MRST2002	GRV98
$C_{\rm hel}$	−0.387	−0.384	−0.328
$C_{\rm beam}$	0.801	0.798	0.735
$C_{\rm off}$	0.808	0.804	0.740
LHC			
$C_{\rm hel}$	0.322	0.315	0.332

corrections are smaller at the LHC than at the Tevatron and vary between 1 and 10%. At both colliders the relative corrections $|(C_{\rm NLO} - C_{\rm LO})/C_{\rm LO}|$ are largest for the all-hadronic decay modes and smallest for the dilepton decay modes.

Table 3 shows the dependence of the NLO results on the choice of the PDFs for dilepton final states. While the results for the CTEQ6 and MRST2002 [15] PDFs agree at the percent level, the GRV98 [14] PDFs give significantly different results at the Tevatron. This is largely due to the fact that the contributions from $q\bar{q}$ and gg initial states contribute to C with opposite signs. This may offer the possibility to constrain the quark and gluon content of the proton by a precise measurement of the double angular distribution (2).

In all results above we used $\mu = m_t = 175$ GeV. A variation of the scale μ between $m_t/2$ and $2m_t$ changes the central results for C at $\mu = m_t$ by roughly ±5%. Varying m_t from 170 to 180 GeV changes the results for C at the Tevatron by less than 5%, while for the LHC, $C_{\rm hel}$ changes by less than a percent.

4 Conclusions

In summary, $t\bar{t}$ spin correlations are large effects that can be studied at the Tevatron and the LHC by measuring double angular distributions both in the dilepton, single lepton and all-hadronic decay channels. The QCD corrections to these distributions are of the order of 10 to 30%. Spin correlations are suited to analyse in detail top quark interactions, search for new effects, and may help to constrain the parton content of the proton.

Acknowledgements. The results presented in this talk have been obtained in collaboration with W. Bernreuther, Z.G. Si and P. Uwer.

References

1. W. Bernreuther, A. Brandenburg, and P. Uwer: Phys. Lett. B **368**, 153 (1996)
2. W.G. Dharmaratna and G.R. Goldstein: Phys. Rev. D **53**, 1073 (1996)
3. W. Beenakker, F.A. Berends, and A.P. Chapovsky: Phys. Lett. B **454**, 129 (1999)
4. W. Bernreuther, A. Brandenburg, Z.G. Si, and P. Uwer: in preparation
5. A. Czarnecki, M. Jezabek, and J.H. Kühn: Nucl. Phys. B **351**, 70(1991)
6. A. Brandenburg, Z.G. Si, and P. Uwer: Phys. Lett. B **539**, 235 (2002)
7. P. Nason, S. Dawson, and R.K. Ellis: Nucl. Phys. B **303**, 607 (1988); Nucl. Phys. B **327**, 49 (1989)
8. W. Beenakker, H. Kuijf, W.L. van Neerven, and J. Smith: Phys. Rev. D **40**, 54 (1989); W. Beenakker et al.. Nucl. Phys. B **351**, 507 (1991)
9. W. Bernreuther, A. Brandenburg, and Z.G. Si: Phys. Lett. B **483**, 99 (2000)
10. W. Bernreuther, A. Brandenburg, Z.G. Si, and P. Uwer: Phys. Lett. B **509**, 53 (2001)
11. G. Mahlon and S. Parke: Phys. Lett. B **411**, 173 (1997)
12. W. Bernreuther, A. Brandenburg, Z.G. Si, and P. Uwer: Phys. Rev. Lett. **87**, 242002 (2001)
13. J. Pumplin et al.: JHEP **0207**, 012 (2002)
14. M. Glück, E. Reya, A. Vogt: Eur. Phys. J. C **5**, 461 (1998)
15. A.D. Martin, R.G. Roberts, W.J. Stirling, and R.S. Thorne: Eur. Phys. J. C **28**, 455 (2003)